Experimental study in heat accumulators with a phase transition of matter

R M Makhmudov[1*], *Z X* Fayziev[1], *Z I* Kholmuradova[1], *M D* Uzboev[1], and *Sh X* Taniberdiyev[1]

[1]Samarkand State University of Architecture and Civil Engineering named after Mirzo Ulugbek, Samarkand, Uzbekistan

Abstract. The proposed article is devoted to the study of a heat accumulator with a phase transition of a substance, which is a model of an accumulator with a semi-co- occupational heat pipe through which a coolant (water) passes at different temperatures. To intensify the heat exchange process between the coolant and the heat-storing material, the tube is fitted with longitudinal and transverse ribs, and aluminum shavings are added to the HSM composition. The experimental results make it possible to suggest that there are such values of the studied parameters (flow rate, coolant temperature) at which a further increase in the latter does not have a significant effect on the rate of processes in heat accumulators based on a phase transition.

1 Introduction

Depending on the nature of the accumulating system intended for research with daily seasonal fluctuations, the accumulation of solar energy can be carried out in exchangeable ways. Among these methods of storing solar energy in the form of electric batteries, earth batteries or chemical energy batteries, etc., the most effective method, apparently, is heat accumulation using heat accumulation with phase change of matter (HAWPCh).

2 Materials and methods

The coolant (water) is heated in the thermostat (Figure 1) by tubular electric heaters and, using pump 7, through control valve 2 and pipeline system 5, is supplied to the model of phase transition heat accumulator 1, from which water returns to the thermostat through rotameter 3. The water temperature in the thermostat is maintained using a contact thermometer 4 and the temperature control range of the water in the thermostat is 20-100 ˚C. The change in coolant flow was achieved using control and bypass valves.

* Corresponding author: bender.zar@gmail.com

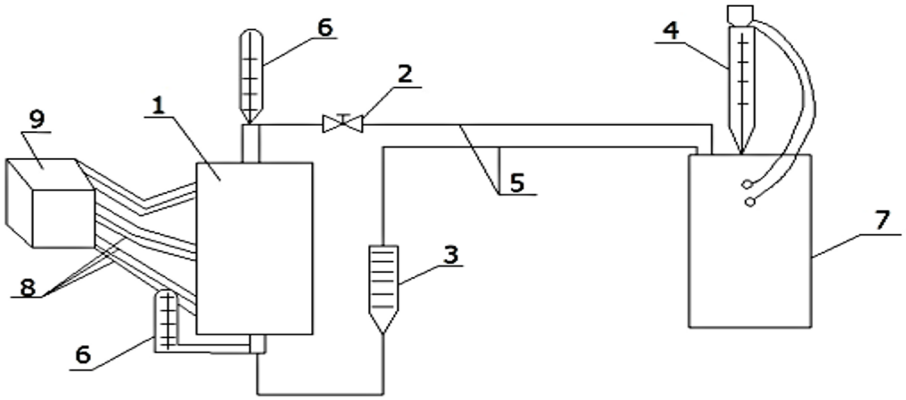

1-model heat accumulator, 2-needle valve, 3-rotameter, 4-contact thermometer, 5-connecting hoses, 6-mercury thermometers, 7-thermostat, 8-chromel-copel (ChC) thermocouples, 9-potentiometer SPC -2

Fig. 1. Schematic diagram of the HAWPCh experimental setup.

The HAWPCh model is a parallelepiped with dimensions: height – 500 mm, width – 110 mm and thickness 24 mm. The model is made of plexiglass 5 mm thick and installed vertically. Inside the model, in the center along the axis, there is a brass pipe with an outer diameter of 16 mm and a wall thickness of 1 mm, through which the coolant is pumped. The space inside the housing was filled with a heat-accumulating substance (HSM) in a molten state. The tube for coolant circulation at the inlet and outlet of the battery model housing was sealed with rubber gaskets. To avoid heat loss to the environment, the outside of the model is covered with a layer of thermal insulation made of polyurethane foam with $\lambda = 0.05$ W/(m.K), 50 mm thick. To visualize the melting process, the thermal insulation on both sides of the model is removable, and at the side, top and bottom ends it remains permanently permanent, and can only be removed at the side walls using handles.

3 Results and Discussion

During the experiments, the following measurements were provided. Using mercury thermometers, the water temperatures at the inlet and outlet of the heating tube were regulated. The division value of these thermometers is -0.1 ˚C. Thermometers in the water flow were installed in special sleeves filled with glycerin and coated on the outside with thermal insulation.

The coolant flow rate was measured with a RM6-04p rotameter with a measurement range of 4-180 kg/hour. The temperature field in HSM was recorded by 12 thermocouples (XK calibration) with a wire diameter of 0.2 mm and a thermocouple ring diameter of 0.3 mm. The thermocouples were located in three sections along the height of the HAWPCh model in the middle of its thickness. In this case, the upper and lower rows of thermocouples were spaced at a distance of 5 mm from the upper and lower ends of the model, respectively. The third row is located exactly in the middle of the height of the model. In each row, one thermocouple was soldered to the tube, and the other three were located every 15 mm from the first. Temperatures were measured and recorded using a twelve-point recording potentiometer SPC -2 with a division value of 1˚C and an accuracy class of 0.5.

n -octodecane and capric acid were used as HSMs in the experiments , the thermophysical characteristics of which are given in Table 1.

Table 1. Some HSMs and their thermal properties.

Metal group	Type, type	Heat storage material	Melting temperature	Latent heat of fusion	
				kJ/kg	10 m^3 kJ/ m^3
I	Hydrates, salts	$CaCl_2 \cdot 6H_2O$	28.5	171	255.8 304.4 321.9 348.8 581.4
		$Zn(NO_3)_2 \cdot 6H_2O$	36	147.4	
		$Na_2S_2O_5 \cdot 5H_2O$	48	201.2	
		$Ni(NO_3)_2 \cdot 6H_2O$	54	187.7	
		$Ba(OH)_2 \cdot 8H_2O$	78	266.7	
II	Acids	Capric	14-16	149	128 135.8 154.9 158.1 158.6 191.3
		Capric	30-32	153	
		Lauric	43-44	178	
		Muristine	53-54	187.3	
		Palmitic	60-62	187.3	
		Stearic	64-66	187.3	
III	Paraffins	P 2001	41-44	189	144.6 145.3 47.3
		P 2002	48-50	189	
		P 2003	62-64	189	

The water in the thermostat was heated to the desired temperature. Then the pump turned on and the heated water began to circulate in the system through the bypass line, bypassing the battery model. At the same time, the required flow rate was set using a rotameter. After this, the water was connected to the battery model and the bypass line was turned off. From this moment the experiment itself began. Temperature measurements in the heat HSM inside the model were carried out continuously and were permanently recorded on the chart tape of the SPC -2 potentiometer. Temperature measurements at the inlet and outlet of the model were carried out every 15 minutes. At the same time,the side heat-insulating covers on the model were removed in order to fix the position of the pressure front. To do this, transparent paper with a coordinate grid was pre-attached to the transparent plexiglass wall, through which the position of the phase transition boundary was clearly visible. On this paper, the position of the phase transition boundary was recorded with a felt-tip pen and the heat-insulating covers were closed.

This measurement was carried out at intervals of 15 minutes until the HSM was completely melted in the HAWPCh model. From this moment on, the hot water from the HAWPCh was turned off and cold water was connected to it. In this case, all measurements continued with the same cyclicity until the HSM completely solidified in the model.

During the experiment, hot water was supplied to the inlet both from below and from above. First, a series of experiments was carried out with lower water supply. In this case, hot water was supplied to the inlet at four temperature levels: 60, 65, 70 and 75 ˚C at a flow rate of 40 kg/h. As a result, a strong dependence of the melting time of the heat-storing material on the temperature of the coolant was revealed (Figure 2); with an increase in the temperature of the coolant, the melting time of the first decreases sharply.

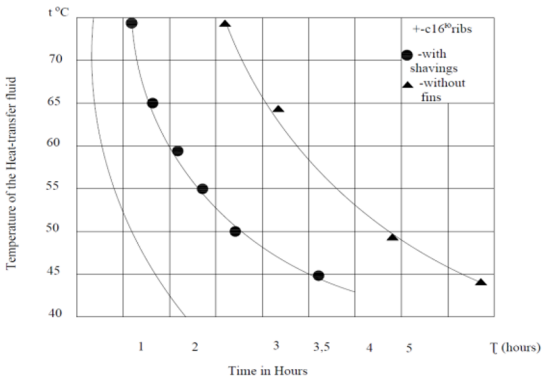

Figure 2

Dependence of the melting time of HSM (capric acid) on the temperature of the coolant at the inlet to the HAWPCh with different designs of heat exchange surfaces

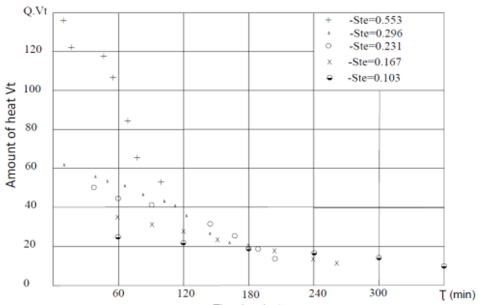

Figure 3

Dependence of the amount of heat transferred to HSM (capric acid) over time τ. Heat exchanger with longitudinal fins $F_{p.n}$=0.15 m²

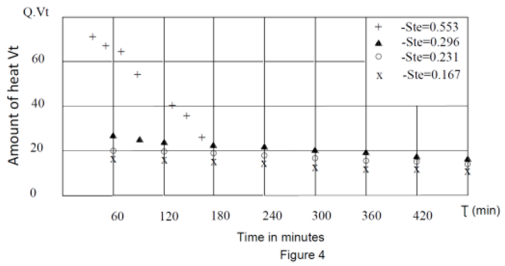

Figure 4

Dependence of the amount of heat transferred to HSM (capric acid) over time τ. Heat exchanger in the form of a smooth tube.

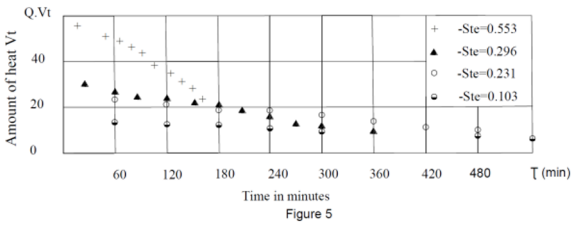

Figure 5

Dependence of the amount of heat transferred to HSM (capric acid) over time τ. The volume (composition) of HSM is aluminum shavings.

Fig. 2. Change in the share of the melt over time, in the presence of aluminum shavings in the battery volume. HSM-paraffin.

However, after a certain value of the coolant temperature, its further increase does not lead to any significant reduction in the melting time. The nature of the advance of the phase transition front indicates a complex mechanism of heat transfer from the walls of the channel with the coolant to the HSM mass. In this case, at the initial moment, heat transfer occurs by thermal conductivity, as evidenced by the fact that the phase transition boundary is equidistant to the walls of the heated channel along the entire height of the HAWPCh. However, over time, the shape of the molten zone begins to deviate from cylindrical. In this case, the speed of movement of the single transition boundary in the upper part of the

HAWPCh significantly exceeds the similar parameter for the lower part. This phenomenon clearly indicates a change in the heat transfer mechanism, namely the appearance of natural convection in the melt, which leads to a distortion of the cylindrical shape of the melt zone. Having obtained, as a result of this series of experiments, an unambiguous and clearly expressed dependence of the melting time of HSM, both on the coolant temperature at the inlet (or, which is basically the same thing, on the difference between the temperature of the wall of the heating channel and the phase transition temperature of HSM) and taking into account that for a real High dynamic characteristics are very important for HAWPCh; it was decided in the future to focus only on elevated coolant temperatures.

The melting time of HSM in HAWPCh on the coolant flow rate was revealed .In this case, the coolant flow was directed from top to bottom, and its inlet temperature in all experiments was maintained at 75. The coolant flow rate was set at four levels: 4, 21, 40 and 180 kg/hour. As a result of experiments, it was found that the melting time of HSM depends quite strongly on the coolant flow rate, although to a much lesser extent on the temperature of the latter at the inlet.

It was also revealed that there is an area of expenses where time melting practically does not depend on the flow rate. Border the value in this case can be considered a flow rate of 40 kg/hour. Comparison HSM melting intensity for different current directions coolant showed that the direction from top to bottom is preferable, since in this case, at the same coolant flow rate, the time for complete melting of HSM in HAWPCh is less (at a flow rate of G = 40 kg/h and the coolant temperature at the inlet to the battery t_{in} = 75 ˚C at current from top to bottom, the time for complete melting was 4 hours 30 minutes, and when moving from bottom to top, it was 6 hours 50 minutes). Based on this, all other experiments were carried out with the coolant moving from top to bottom.

When the melt solidified, the picture seemed to be inverted; the volume of the solidifying phase around the channel with cold water constantly increased from top to bottom along the flow of the cold coolant. At the same time, with an increase in flow rate at a constant temperature of the cold coolant, the solidification time of HSM also decreases. However, the deviation of the shape of the solidification zone from the cylindrical one is less pronounced than the melt zone during melting. In addition, after a certain time from the beginning of the solidification process, the phase transition boundary is blurred and it becomes impossible to clearly determine its position visually, which is due to the design features of the HAWPCH model, namely: when removing the front heat-insulating cover to fix the position of the solidification front, the melt is cooled through the plexiglas the wall of the model and on the inner surface of the latter, as a result, a layer of hardened HSM (paraffin or capric acid) appears, which is not transparent. Under these conditions, the completion of the solidification process was recorded according to the readings of thermocouples (inside the HAWPCh).

The temperature according to the readings of all thermocouples should be below the phase transition temperature. The direction of movement of the coolant affects the rate of solidification and, to a lesser extent, the shape of the resulting crystallization zone.

4 Conclusion

It has been revealed that the movement of the cooling fluid from bottom to top is more effective than from top to bottom. In this case, the indication of the cylindrical shape of the crystallization zone around the cooled channel is more significant. Further, as a result of an increase in the density of the solid phase relative to the liquid, the upper boundary of the HSM in the battery drops, and a hard crust of hardened HSM forms on it with any movement in the direction of the coolant, which constantly thickens. Thus, HSM

crystallization in HAWPCh occurs not only around the cooling channel, but also from top to bottom from the upper boundary of the melt into the latter.

Analysis of the results of the preliminary experimental study allowed us to draw the following conclusions. It is preferable to supply coolant from top to bottom. Moreover, even in the case of low coolant flow rates at a sufficiently high temperature, the melting time is well within daylight hours. Solidification of the melt occurs faster than melting. Perhaps this factor is due to the fact that the difference between the temperature of the phase transition and the temperature of the hot coolant in the case of melting was less than the same difference relative to the temperature of the cold coolant in the case of solidification.

Further, the experimental results make it possible to suggest that there are such values of the studied parameters (flow rate, coolant temperature) at which a further increase in the latter does not have a significant effect on the rate of processes in heat accumulators based on a phase transition. Visual observations of the melting process made it possible to establish the rather interesting fact of recrystallization of paraffin when it is heated to temperatures close to the phase transition temperature. From an amorphous opaque state before melting, paraffin passes into a glassy translucent state and only after that melts. As a result, upon visual observation, two fronts are clearly visible —the melting front, and in front of it, at a distance of about a centimeter deep into the solid phase, the crystallization front. It is assumed that to a certain extent this nature of the process , apparently associated with the complex component composition of paraffin's, is also reflected in the thermal characteristics of ATPP. During the reverse process of solidification, such a clearly defined picture is not observed, however, chaotically located zones with different densities of the solid phase are clearly distinguished.

The next stage of the experimental program was to study the effect of fins on the intensity of processes in ATPP. Due to the design features of the HAWPCH model, only transverse fins were studied. The fins were made of copper 1 mm thick. The number of fins in the experiments varied discretely - 1, 3, 8, 17, to which the heating surfaces correspond - 0.0083 m^2, 0.0249 m^2, 0.0664 m2 , 0.1412 m^2. At the same time, for a design with one rib, a series of experiments was carried out with different flow rates (4, 21, 40 kg/h, and for 17 ribs, at flow rates of 4 and 40 kg/h). During the experiments, the coolant temperature was 75 ˚C.

Accepted abbreviations

SPC - Self-recording potentiometric compensator.
HSM – heat-storing material.
HAWPCh–heat accumulators with phase change.
Ste–Stefan number Ste =cΔt / Δin
C – is the specific heat capacity of the substance, KJ=k/kg*s
Δt- temperature difference between melting point of the material, ºC
Δi- latent heat of fusion, kJ/

References

1. G. Beckman, P.V. Gilley, Thermal accumulation of energy (Mir, Moscow, 1987)
2. V.D. Levenberg, Heat accumulation (Technology, Kyiv, 1991)
3. R. Viskanta, Heat transfer during melting and solidification of metals, Modern mechanical engineering Series A, **6**, 119-139 (1989)

4. M.I. Kukolev, Fundamentals of design of thermal energy storage devices, Petrozavodsk (2001)
5. O.A. Sotnikov, Heat accumulators of heat generating installations of heat supply systems, ABOK magazine, **5** (2003)
6. R. Makhmudov, Heat accumulators with phase transition of heat-storing material for heat supply systems, Abstract of the dissertation K (1990)
7. Z. Kh. Fayziev, Pressure losses in Venturi pipes, their rational forms and coefficients of local resistance, 2762 (2022) https://doi.org/10.1063/5.0128505
8. Y.K. Rashidov, J.T. Orzimatov, K.Y. Rashidov, Z.X. Fayziev, The Method of Hydraulic Calculation of a Heat Exchange Panel of a Solar Water-Heating Collector of a Tube–Tube Type with a Given Nonuniform Distribution of Fluid Flow Along Lifting Pipes. Applied Solar Energy (English Translation of Geliotekhnika), **56**, **1**, 30–34 (2020) https://doi.org/10.3103/S0003701X20010107